Chiral phase transition in the presence of spinodal decomposition

C. Sasaki,[1] B. Friman,[2] and K. Redlich[3,4]

[1]Technische Universität München, D-85748 Garching, Germany
[2]Gesellschaft für Schwerionenforschung, GSI, D-64291 Darmstadt, Germany
[3]Institute of Theoretical Physics, University of Wroclaw, PL–50204 Wrocław, Poland
[4]Institute für Kernphysik, Technische Universität Darmstadt, D-64289 Darmstadt, Germany

(Dated: February 2, 2008)

The thermodynamics of a first order chiral phase transition is considered in the presence of spinodal phase separation within the Nambu-Jona-Lasinio (NJL) model. The properties of the basic thermodynamic observables in the coexistence phase are discussed for zero and non-zero quark masses. We focus on observables that probe the chiral phase transition. In particular, the behavior of the specific heat and entropy as well as charge fluctuations are calculated and analyzed. We show that the specific heat and charge susceptibilities diverge at the isothermal spinodal lines. We determine the scaling behavior and compute the critical exponent γ of the net quark number susceptibility at the isothermal spinodal lines within the NJL model and the Ginsburg-Landau theory. We show that in the chiral limit the critical exponent $\gamma = 1/2$ at the tricritical point as well as along the isothermal spinodal lines. On the other hand, for finite quark masses the critical exponent at the spinodal lines, $\gamma = 1/2$, differs from that at the critical end point, $\gamma = 2/3$, indicating a change in the universality class. These results are independent of the particular choice of the chiral Lagrangian and should be common for all mean field approaches.

PACS numbers: 25.75.Nq, 24.60.Lz

1. INTRODUCTION

A first order phase transition is intimately linked with the existence of a convex anomaly in thermodynamic pressure [1], which can be probed only in non-equilibrium states. There is an interval of energy and/or baryon number density where the derivative of pressure with respect to the volume of the system is positive. This anomalous behavior defines a region of instability in the (T, n_q)-plane with n_q being the net quark number density. The region is bounded by the spinodal lines, where the pressure derivative with respect to volume vanishes. The derivative taken at constant temperature or entropy defines the isothermal and isentropic spinodal lines, respectively. Spinodal decomposition is thought to play a dominant role in the dynamics of low energy nuclear collisions in the regime of the first order nuclear liquid-gas transition [1, 2]. Furthermore, the consequences of spinodal decomposition in the connection with the chiral and deconfinement phase transitions in heavy ion collisions have been discussed in Refs. [1, 2, 3, 4, 5, 6]. It has been argued that in the region of phase coexistence, a spinodal phase separation leads to a significant enhancement of baryon [3] and strangeness fluctuations [4]. Studies of non-equilibrium dynamics in the linear sigma model have shown that significant density inhomogeneities may be dynamically induced in a first-order chiral phase transition [7]. In a recent paper it was shown that the spinodal instability is connected with divergent fluctuations of the net quark number, $\langle N_q N_q \rangle - \langle N_q \rangle \langle N_q \rangle = VT\chi_q$, along the isothermal spinodal lines [8]. Consequently, the quark number susceptibility χ_q diverges not only at the critical end point (CEP) in the QCD phase diagram but also at the (non-equilibrium) first order phase transition. The close relation of the singularities at the CEP with those at the spinodal lines is a consequence of the thermodynamic relations connecting the compressibility of the system with the quark number susceptibility. In this paper we explore the critical behavior and properties of the fluctuations of conserved charges and the specific heat in the presence of spinodal phase decomposition using the Nambu-Jona-Lasinio (NJL) model. In particular, we study the influence of an explicit chiral symmetry breaking through the finite value of the quark mass on the thermodynamics across the off-equilibrium first order transition. The critical exponents of χ_q at the CEP and along the spinodal lines are computed in the NJL model and in the Ginzburg-Landau effective theory. In the chiral limit, the critical exponents at the CEP and at the spinodal lines are identical, while for finite vales of the quark mass, the exponents differ. Our calculations are done within the mean-field approximation to the NJL model. However, the results are generic and should apply to all QCD-like chiral models. We stress at this point that for non-universal quantities, like the position of the CEP, one can expect only qualitative agreement between different models. On the other hand, for universal quantities, like the critical exponents, all models in the same universality class yield the same result #1.

The paper is organized as follows: In Section 2 we explore the general features of the spinodal instabilities within the NJL model. In Section 3 we discuss the critical behavior of the quark number susceptibility in the

#1 The critical exponents obtained in the mean-field approximation are in general modified by fluctuations.

mean field approximation. The critical exponents of χ_q are computed in Ginzburg-Landau theory in Section 4. Concluding remarks are presented in Section 5.

2. EFFECTIVE CHIRAL MODEL AND SPINODAL INSTABILITIES

We study the thermodynamics of the chiral phase transition in the presence of spinodal instabilities within the Nambu–Jona-Lasinio (NJL) model [9]. The model describes the effective interactions of quarks preserving the chiral symmetry of the massless QCD Lagrangian. We include quark interactions only in the scalar and isoscalar sectors. In this case the NJL Lagrangian for two quark flavors, three colors and for finite quark chemical potentials has the form [10, 11, 12, 13]:

$$\mathcal{L} = \bar\psi(i\partial\!\!\!/ - m)\psi + \bar\psi\mu_q\gamma_0\psi + G_S\Big[\big(\bar\psi\psi\big)^2 + \big(\bar\psi i\vec\tau\gamma_5\psi\big)^2\Big] , \tag{2.1}$$

where $m = \mathrm{diag}(m_u, m_d)$ is the current quark mass, $\mu_q = \mathrm{diag}(\mu_u, \mu_d)$ is the quark chemical potential and $\vec\tau$ are Pauli matrices. The strength of the interactions among the constituent quarks is controlled by the coupling $G_S\Lambda^2 = 2.44$ with the three momentum cut-off $\Lambda = 587.9$ MeV, introduced to regulate the ultraviolet divergences [10]. The parameters of the model are fixed so as to reproduce the pion mass and decay constant in vacuum for $m_u = m_d = 5.6$ MeV.

In the mean field approximation the thermodynamics of the NJL model, for an isospin symmetric system, is obtained from the thermodynamic potential [10]:

$$\Omega(T,\mu;M)/V = \frac{(M-m)^2}{4G_S} - 12\int\frac{d^3p}{(2\pi)^3}\Big[E(\vec p) - T\ln(1-n^{(+)}(\vec p,T,\mu)) - T\ln(1-n^{(-)}(\vec p,T,\mu)\Big] , \tag{2.2}$$

where $M = m - 2G_S\langle\bar\psi\psi\rangle$ is the dynamical quark mass, $E(\vec p) = \sqrt{\vec p^2 + M^2}$ is its energy and $n^{(\pm)}(\vec p,T,\mu) = \Big(1+\exp\big[(E(\vec p)\mp\mu)/T\big]\Big)^{-1}$ is the particle/antiparticle distribution function. The quark chemical potential μ is expressed as an average $\mu = \mu_u = \mu_d$. The dynamical quark mass M in Eq. (2.2) is obtained self-consistently from the stationarity condition $\partial\Omega/\partial M = 0$, which implies:

$$M = m + 24G_S\int\frac{d^3p}{(2\pi)^3}\frac{M}{E}\Big[1 - n^{(+)} - n^{(-)}\Big] . \tag{2.3}$$

The thermodynamic pressure of the system is given by $P = -\Omega/V$, and the net quark number density n_q is given by

$$n_q = \frac{\partial P}{\partial\mu} = 12\int\frac{d^3p}{(2\pi)^3}\Big[n^{(+)} - n^{(-)}\Big] . \tag{2.4}$$

Thus, in the mean-field approximation the net quark density n_q has the same structure as in a non-interacting gas of massive fermions, albeit with a (T,μ)-dependent effective mass $M(T,\mu)$. The dynamical quark mass M is an order parameter of the chiral phase transition. In the left panel of Fig. 1 we show M computed at fixed temperature $T = 30$ MeV as a function of the quark chemical potential, in the chiral limit, i.e., for vanishing current quark masses. The behavior of M is typical for an order parameter in a first order phase transition. There is a range of values of the chemical potential where there are several solutions to the gap equation. There are stable/metastable solutions, corresponding to absolute/local minima of the thermodynamic potential and an unstable solution, corresponding to a maximum. The equilibrium transition from the chirally broken to the symmetric phase is obtained when the two minima are degenerate. This corresponds to the so called Maxwell construction. The location of the equilibrium transition is indicated in Fig. 1 by the dashed line. A non-zero current quark mass in the NJL Lagrangian explicitly breaks the chiral symmetry. Consequently, in this case, the dynamical mass M is not a true order parameter and it never vanishes. The dependence of M on the quark chemical potential is shown in the right panel of Fig. 1. The characteristic dependence of M on the chemical potential at a first order transition is, as will be discussed below, reflected in various thermodynamic quantities.

In Fig. 2 we show the net quark number density at fixed temperature as a function of μ for vanishing as well as for a finite current quark mass. As expected, the non-monotonic dependence of the mass M on the chemical potential results in corresponding structure in n_q. However, there is an notable difference in the properties of n_q in the chiral limit and for a finite quark masses. In the latter case, n_q is differentiable at all values of μ, while in the chiral limit n_q exhibits a cusp at the point where the dynamical quark mass vanishes. This has important consequences for observables obtained from n_q through differentiation with respect to thermal parameters, like e.g. the quark number or mixed susceptibilities. The thermodynamic pressure as a function of the volume per net quark, $(1/n_q)$, is shown in Fig. 3 at fixed temperature. Independently of the current quark mass, the qualitative structure of the pressure is that of a van-der-Waals' equation of state. The unstable solution of the gap equation corresponds to the part of the equation of state where the volume derivative of the pressure is positive, i.e., to the mechanically unstable region. This region is bounded by the spinodal points located at the minimum and maximum of the pressure, respectively. Outside of this region the system is mechanically stable [#2]. The volume deriva-

---

[#2] More precisely, the system is absolutely stable outside the coexistence region, while within this region but outside the spinodal lines it is metastable, i.e., stable only against small amplitude

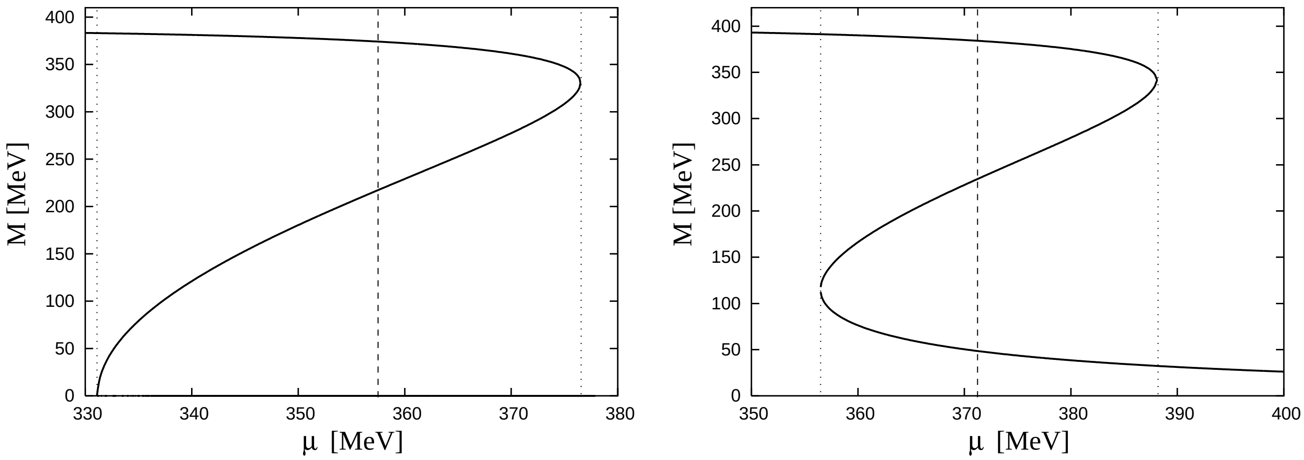

FIG. 1: The dynamical quark mass at fixed temperature ($T = 30$ MeV) as a function of the quark chemical potential in the chiral limit (left panel) and for a finite quark mass $m = 5.6$ MeV (right panel). The dashed line indicates the equilibrium first order phase transition while the dotted lines show the isothermal spinodal points.

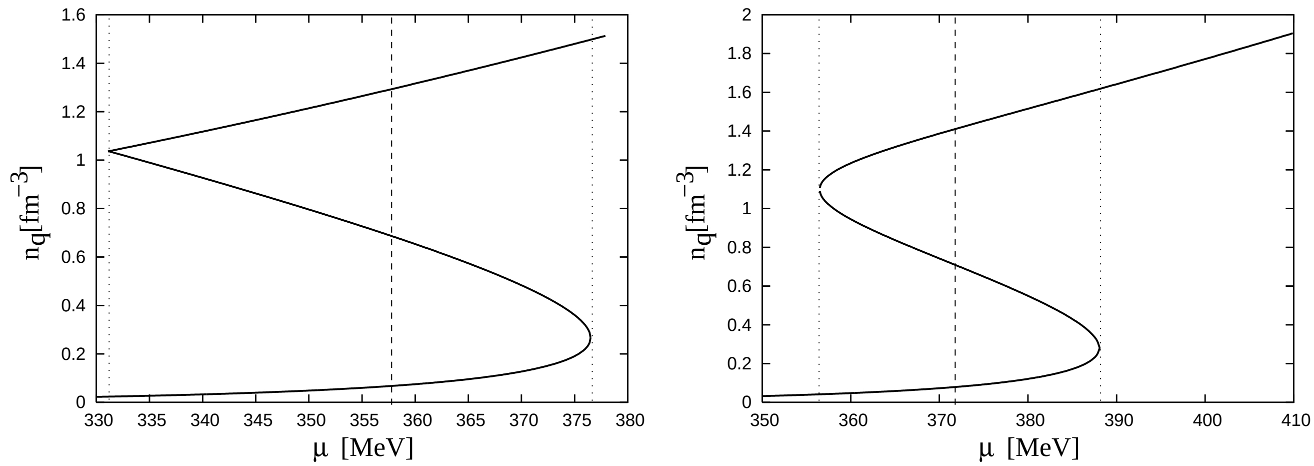

FIG. 2: The net quark number density at $T = 30$ MeV computed in the chiral limit (left panel) and for a finite quark mass $m = 5.6$ MeV (right panel). The dashed and dotted lines have the same meaning as in Fig. 1.

tive of the pressure depends on which quantity is kept constant, the temperature or the entropy. If the volume derivative of P exists, then the isothermal and isentropic spinodal lines are defined by zeroes of the corresponding derivatives

$$\left(\frac{\partial P}{\partial V}\right)_T = 0 \qquad \text{or} \qquad \left(\frac{\partial P}{\partial V}\right)_S = 0\,. \tag{2.5}$$

From Fig. 3, it is clear that for a finite quark mass m, the derivative of the thermodynamic pressure is well defined everywhere. However, in the chiral limit the pressure exhibits a cusp rather than a regular minimum, at the point where the pressure derivative changes sign on the high density side. Consequently, in this case equation (2.5) can not be used to determine the position of the spinodal line. Instead, the corresponding branch of the isothermal or isentropic spinodal line is defined by a change in sign of the pressure derivative, or equivalently by a minimum of the pressure. As we discuss below, the corresponding singularity of the thermodynamic potential is weaker than at a regular spinodal line. In Fig. 4 the phase diagram of the NJL model in the (T, n_q) plane is shown, including the isentropic and isothermal spinodal lines. For finite m the NJL model yields a generic phase diagram with a first-order phase transition at low temperatures and high densities and a cross-over transition at high temperatures. The critical end point separates the cross-over from the first-order transition. In the chiral limit, the

fluctuations.

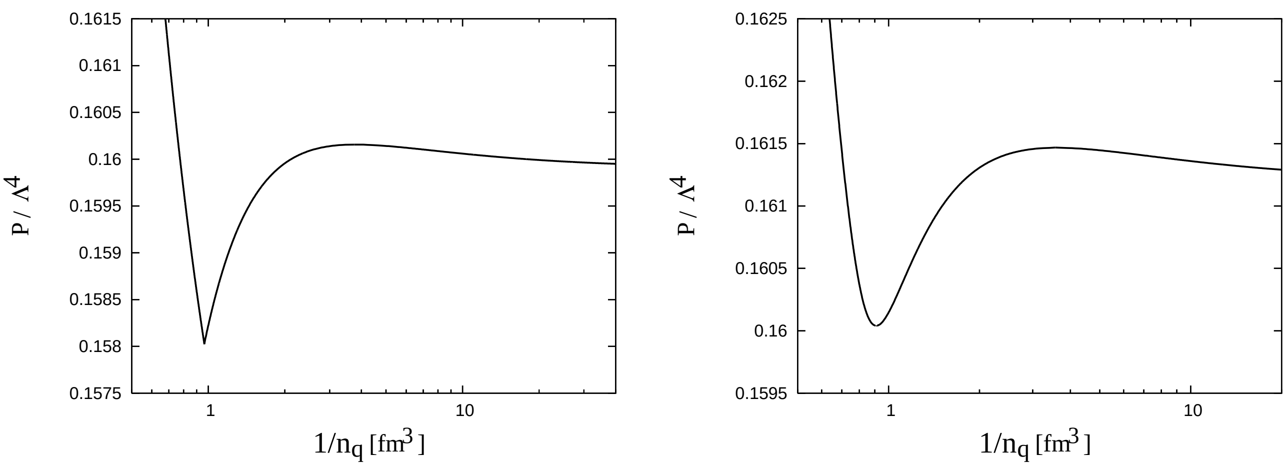

FIG. 3: In the left panel we show the pressure as a function of inverse quark number density for fixed temperature, $T = 30$ MeV obtained in the chiral limit, while in the right panel we show the results for a finite quark mass, $m = 5.6$ MeV.

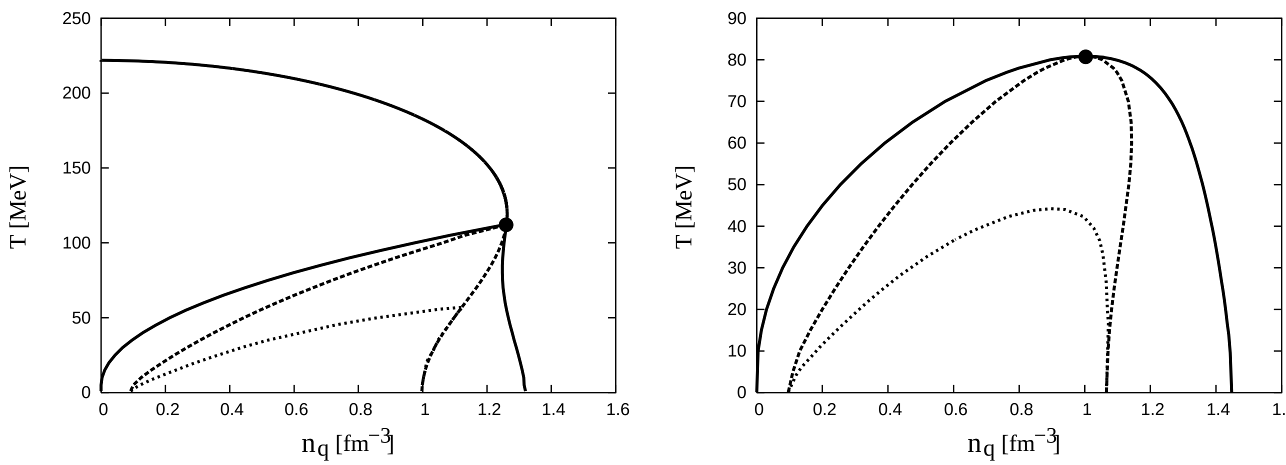

FIG. 4: The phase diagram of the NJL model in (T, n_q)-plane. The left figure corresponds to the chiral limit. The dot indicates the position of the TCP and the full-line above the TCP shows the second order transition line. The full-lines below the TCP represent the phase boundaries of the first order chiral transition. Finally, the dashed (dotted) lines show the isothermal (isentropic) spinodal lines. The right figure was computed with a finite quark mass $m = 5.6$ MeV. Above the CEP, indicated by a dot, there is cross-over transition.

cross-over transition becomes a second-order phase transition. In an equilibrium first-order phase transition, the meta-stable and unstable regions are not probed. The states of maximum entropy, obtained by the Maxwell construction, correspond to the coexistence of the high- and low-density states at the corresponding phase boundaries. On the other hand, in a non-equilibrium system, where the thermal parameters are changing sufficiently fast, the system may traverse the meta-stable and enter the unstable region, bounded by the spinodal lines. From the thermodynamic relation

$$\left(\frac{\partial P}{\partial V}\right)_T = \left(\frac{\partial P}{\partial V}\right)_S + \frac{T}{C_V}\left[\left(\frac{\partial P}{\partial T}\right)_V\right]^2, \qquad (2.6)$$

it is clear that the isentropic spinodal lines are located inside the isothermal spinodal region and furthermore, that the two lines coincide at $T = 0$. As shown in Fig. 4, the isothermal spinodal lines join at the CEP, whereas the boundary of the isentropic spinodal region remains well below the CEP. The latter property is probably an artefact of the mean-field approximation. When fluctuations are included, the specific heat at constant volume C_V diverges at the CEP, although with a weaker singularity than C_P, while in the mean-field approximation C_V remains finite (see section 3). According to (2.6) the isentropic and isothermal volume derivatives of the pressure are equal for $C_V \to \infty$. This implies that also $\partial P/\partial V|_S = 0$ at the CEP and that the isentropic spin-

odal region probably extends to the CEP. In order to explore this question in more detail and to determine the shape of the isentropic spinodal region, a systematic study of fluctuations is required. At a first-order phase transition the instabilities are reflected in a convex structure of several thermodynamic functions. Such a structure is seen in the thermodynamic pressure and also appears in the entropy density as a function of quark density n_q

$$\begin{aligned} s &= -\frac{\partial \Omega}{\partial T} \\ &= -2N_cN_f \int \frac{d^3p}{(2\pi)^3}\Big[\ln(1-n_f^{(+)}) + \ln(1-n_f^{(-)}) \\ &\quad - \frac{E_f}{T}\left(n_f^{(+)}+n_f^{(-)}\right) + \frac{\mu}{T}\left(n_f^{(+)}-n_f^{(-)}\right)\Big]. \qquad (2.7) \end{aligned}$$

However, the entropy per quark, s/n_q, exhibits a monotonic dependence on the density. In Fig. 5 we show s/n_q computed at fixed temperature in the chiral limit and for a finite quark mass. In the chiral limit the entropy per quark shows a cusp structure at the spinodal line on the high-density side.

3. SUSCEPTIBILITIES AND THE CRITICAL BEHAVIOR

At the critical end point the fluctuations of the quark density diverge [14, 15, 16, 17, 18, 19], while they are finite above and below the CEP if the first order transition takes place in equilibrium. However, in non-equilibrium the system may reach the spinodal instability. It is thus natural to explore the charge fluctuations in the metastable and unstable regions of the first order phase transition. In statistical systems a measure of the fluctuations of a particular quantity is provided by the corresponding susceptibility χ. This are obtained as second derivative of the thermodynamic pressure. For the characterization of the spinodal region of the first order chiral phase transition, the susceptibilities related to the net quark number density $\chi_q \equiv \chi_{\mu\mu}$, electric charge density χ_Q as well as the thermal χ_{TT} and mixed $\chi_{\mu T}$ susceptibilities are of particular interest. These are obtained from the thermodynamic pressure (2.2) as follows:

$$\begin{aligned} \chi_{\mu\mu} &= -\frac{\partial^2\Omega}{\partial\mu^2} \\ &= \frac{2N_cN_f}{T}\int\frac{d^3p}{(2\pi)^3}\left[\left(1-\frac{M}{E}\frac{\partial M}{\partial\mu}\right)n^{(+)}(1-n^{(+)}) + \left(1+\frac{M}{E}\frac{\partial M}{\partial\mu}\right)n^{(-)}(1-n^{(-)})\right], \qquad (3.1) \\ \chi_{\mu T} &= -\frac{\partial^2\Omega}{\partial\mu\partial T} \\ &= \frac{2N_cN_f}{T^2}\int\frac{d^3p}{(2\pi)^3}\left[\left(1-\frac{M}{E}\frac{\partial M}{\partial\mu}\right)(E-\mu)\,n^{(+)}(1-n^{(+)}) - \left(1+\frac{M}{E}\frac{\partial M}{\partial\mu}\right)(E+\mu)\,n^{(-)}(1-n^{(-)})\right], \qquad (3.2) \\ \chi_{TT} &= -\frac{\partial^2\Omega}{\partial T^2} \\ &= \frac{2N_cN_f}{T^2}\int\frac{d^3p}{(2\pi)^3}\left[\left(\frac{E-\mu}{T}-\frac{M}{E}\frac{\partial M}{\partial T}\right)(E-\mu)\,n^{(+)}(1-n^{(+)}) + \left(\frac{E+\mu}{T}-\frac{M}{E}\frac{\partial M}{\partial T}\right)(E+\mu)\,n^{(-)}(1-n^{(-)})\right]. \qquad (3.3) \end{aligned}$$

The susceptibilities involve derivatives of the dynamical quark mass with respect to μ or T [#3]. Consequently, at the spinodal lines, where both $\partial M/\partial\mu$ and $\partial M/\partial T$ diverge (see Fig. 1), one expects singularities in these susceptibilities. In Fig. 6 we show the quark number susceptibility as a function of n_q at a fixed temperature $T = 30$ MeV. As expected, it is singular at the spinodal points. However, in the chiral limit the susceptibility exhibits only a weak singularity at the high-density point, corresponding to the cusp in the pressure in Fig. 3. At this point the susceptibility is discontinuous, changing from a finite negative to a finite positive value, while at the low density spinodal point the susceptibility diverges, corresponding to very large fluctuations of the net quark density. Moreover, for a finite current quark mass, the

[#3] The above form of the mixed susceptibility is obtained from $\chi_{\mu T} = \partial s/\partial\mu$. An alternative equation, involving $\partial M/\partial T$, is obtained from $\chi_{\mu T} = \partial n_q/\partial T$. The equivalence of the two is obvious when the explicit expressions for $\partial M/\partial\mu$ and $\partial M/\partial T$ are inserted.

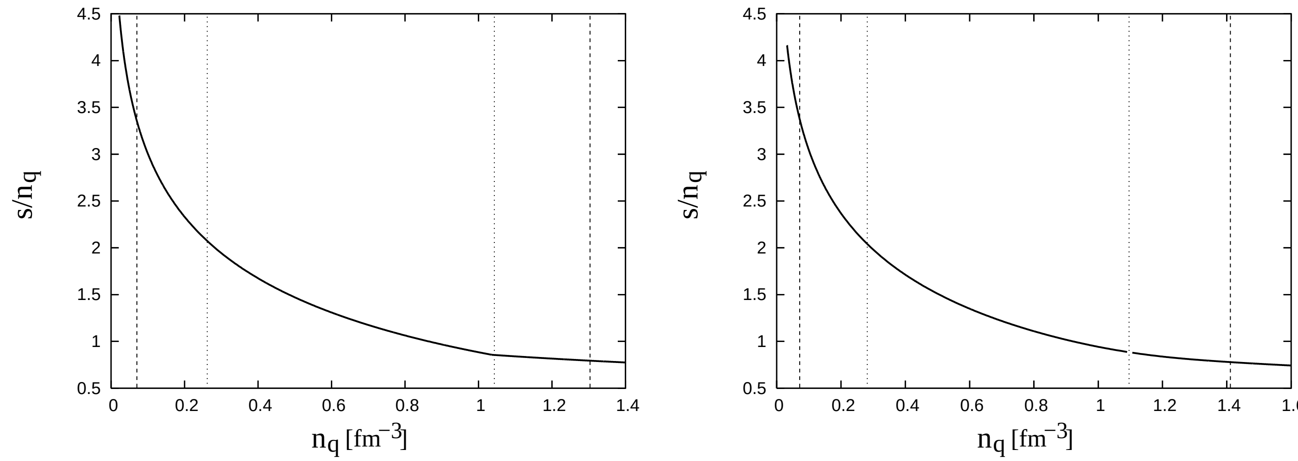

FIG. 5: The ratio of the entropy to the net quark number density, i.e., the entropy per quark, at fixed temperature as a function of the net quark density in the chiral limit (left panel) and for a finite quark mass $m = 5.6$ MeV (right-panel). The dashed and dotted lines have the same meaning as in Fig. 1.

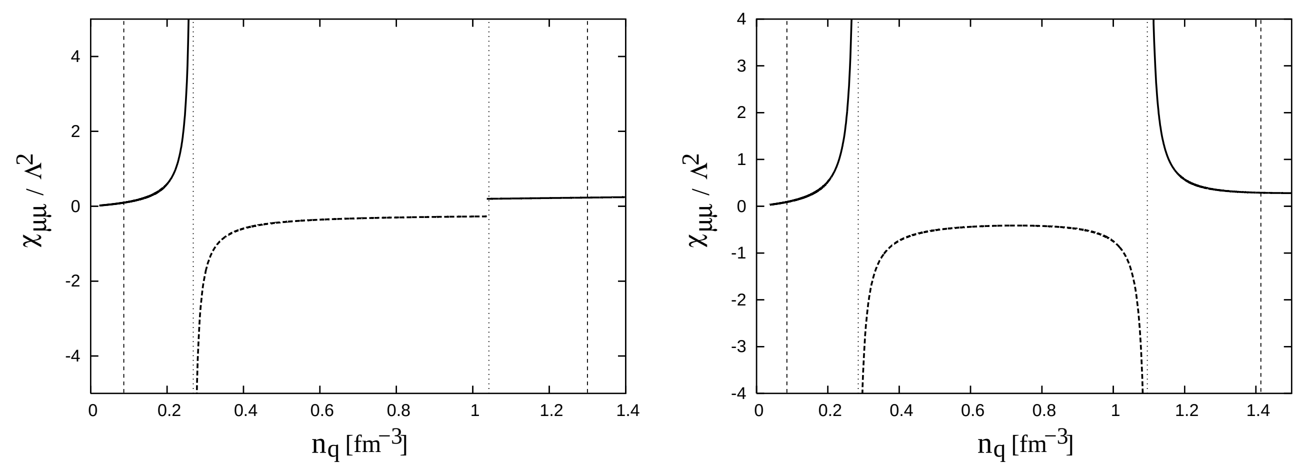

FIG. 6: The $\chi_{\mu\mu}$ susceptibility at fixed temperature $T = 30$ MeV in the chiral limit (left panel) and for a finite quark mass $m = 5.6$ MeV (right panel). The vertical dashed and dotted lines have the same meaning as in Fig. 1.

susceptibility diverges at both spinodal points. In both cases the quark number susceptibility is negative in the spinodal region, indicating a mechanical instability of the system.

The critical properties of the net quark number susceptibility seen at the isothermal spinodal lines are not there along the isentropic spinodal trajectories. There, the susceptibilities are finite and continues when the system passes through the metastable region. The above behavior of $\chi_{\mu\mu}$ appears as a direct consequence of the thermodynamic relations

$$\left(\frac{\partial P}{\partial V}\right)_T = -\frac{n_q^2}{V}\frac{1}{\chi_{\mu\mu}}\,, \tag{3.4}$$

$$\left(\frac{\partial P}{\partial V}\right)_S = -\frac{n_q^2}{V}\frac{\chi_{TT} - \frac{2s}{n_q}\chi_{\mu T} + \left(\frac{s}{n_q}\right)^2\chi_{\mu\mu}}{\chi_{\mu\mu}\chi_{TT} - \chi_{\mu T}^2}\,, \tag{3.5}$$

that connect the pressure derivatives with the susceptibilities $\chi_{xy} = -\partial^2\Omega/\partial x\partial y$.

Along the isothermal spinodal lines the pressure derivative in Eq. (3.4) vanishes. Thus, for non vanishing density n_q its fluctuations have to diverge. In addition, since the pressure derivative $\partial P/\partial V|_T$ changes its sign when crossing the spinodal trajectories, there is a corresponding sign change of the divergence in $\chi_{\mu\mu}$ as seen in

Fig. 6. A similar behavior as for $\chi_{\mu\mu}$ is also expected for electric charge χ_Q, strangeness χ_S or isovector χ_I fluctuations if their charge densities are finite.

In heavy ion collisions the isospin asymmetry is usually negligible at high energy and the strangeness density vanishes due to strangeness neutrality in the initial state. Thus, here not all chemical potentials are thermodynamically independent. The net quark number $\chi_q = -\partial^2\Omega/\partial\mu_q^2$ and the isovector $\chi_I = -\partial^2\Omega/\partial\mu_I^2$ susceptibilities are related with the electric charge fluctuations χ_Q as

$$\chi_Q = \frac{1}{36}\chi_q + \frac{1}{4}\chi_I + \frac{1}{6}\frac{\partial^2 P}{\partial\mu_q\partial\mu_I}\,, \tag{3.6}$$

For isospin symmetric system the derivative of the pressure vanishes and all relevant susceptibilities are linearly dependent. Clearly, since χ_q diverges on the isothermal spinodals and since $n_I \simeq 0$ is a good approximation in heavy ion collisions, thus the electric charge fluctuations χ_Q should show similar critical behavior to that seen in χ_q. On the isentropic spinodals the quark number fluctuations are finite. This is also valid for all mixed susceptibilities appearing in Eq. (3.5). The isentropic condition (2.5) holds since the numerator in (3.5) vanishes. The exception is the point at $T = 0$ where the isothermal and isentropic spinodal conditions are equivalent since the entropy density and the $\chi_{\mu T}$ vanish at $T = 0$. The thermal χ_{TT} and mixed $\chi_{\mu T}$ susceptibilities along the isothermal spinodals show similar critical behavior as found for $\chi_{\mu\mu}$ in Fig. 6. When going beyond the mean field dynamics, the isothermal and the isentropic spinodal curves could also coincide at the CEP. Thus, from Eqs. (3.4) and (3.5) it is clear that all susceptibilities should diverge at the CEP in this case.

For equilibrium first order phase transition the properties of charge fluctuations are different from those seen in Fig. 6. There, under the mean field approximation, the charge susceptibilities are positive and exhibit a discontinuity at the transition point [20, 21]. This discontinuous structure is eventually converted to a cusp if the quantum correction are included [21, 22]. However, the essential difference is that the susceptibilities in the equilibrium transition are finite whereas they are divergent if spinodal phase separation appears.

The rate of change in entropy with respect to temperature at constant volume or pressure gives the specific heat expressed as

$$C_V = T\left(\frac{\partial S}{\partial T}\right)_V = TV\left[\chi_{TT} - \frac{\chi_{\mu T}^2}{\chi_{\mu\mu}}\right]\,, \tag{3.7}$$

$$C_P = T\left(\frac{\partial S}{\partial T}\right)_P = TV\left[\chi_{TT} - \frac{2s}{n_q}\chi_{\mu T} + \left(\frac{s}{n_q}\right)^2\chi_{\mu\mu}\right]. \tag{3.8}$$

From Eqs. (3.5), (3.7) and (3.8) it is clear that the ratio of specific heats C_P/C_V satisfies a well known relation

$$\left(\frac{\partial P}{\partial V}\right)_S = \frac{C_P}{C_V}\left(\frac{\partial P}{\partial V}\right)_T. \tag{3.9}$$

In Fig. 7 we show the specific heat C_V at fixed temperature. One sees in the chiral limit a discontinuity at the right-handed spinodal branch which comes from a similar jump in χ_{xy}. At the left-handed spinodal branch C_V is continuous and finite. Each susceptibility χ_{xy} diverges at the spinodal point, however such singularities are canceled out in Eq. (3.7). The above is also valid for finite quark masses, thus C_V continuously changes at both spinodals.

On the other hand, as seen in Fig. 8, the C_P diverges at the isothermal spinodals because there is no cancellation of the singularities among χ_{xy} in Eq. (3.8). It has been argued that the negative specific heat could be a signal of the liquid-gas phase transition [23] and its occurrence has recently been reported as the first experimental evidence for such an anomalous behavior in low-energy nuclear collisions [24, 25].

From Eqs. (3.5) and (3.8) one finds that C_P vanishes along the isentropic spinodal lines. However, this is not the case in the chiral limit. Here the pressure shows a cusp, thus its derivative is not defined. Consequently, $\partial P/\partial V|_S$ is non-vanishing at this isentropic spinodal line and C_P remains finite.

At the CEP the fluctuations of charge densities that couple to the massless modes of the sigma field are divergent. Fig. 9 shows the $\chi_{\mu\mu}$ near the CEP and at fixed temperature corresponding to the first order transition. From this figure it is clear that when approaching the CEP from the side of the first order transition the region of instabilities shrinks and at the CEP disappears completely. Consequently, the CEP singularity in $\chi_{\mu\mu}$ appears from the matching of the two positive singular branches of $\chi_{\mu\mu}$. The strength of the singularity is controlled by the critical exponent γ shown in Fig. 10. In the chiral limit the exponent at the isothermal spinodal line is identical to that at the TCP. From numerical analysis we find that $\chi_{\mu\mu} \sim (\mu - \mu_c)^{-\gamma}$, with $\gamma = 1/2$. However, for finite quark masses we find $\gamma = 2/3$ at CEP, in agreement with that expected in the mean-field approximation [21, 22]. From the numerical studies of $\chi_{\mu\mu}$ at spinodals we found that $\gamma = 1/2$ independently of the value of the quark mass. Thus, the singular properties at the TCP/CEP are the remnant of divergent behavior of the $\chi_{\mu\mu}$ at the first order chiral phase transition [8]. Clearly, the critical exponents are renormalized by quantum fluctuations [22]. However, the smooth evolution of the singularity from the spinodal lines to the CEP is expected to be generic.

In the next section we disuse how the critical exponents of quark susceptibilities along the spinodal lines can be analytically justified within the Ginzburg-Landau theory.

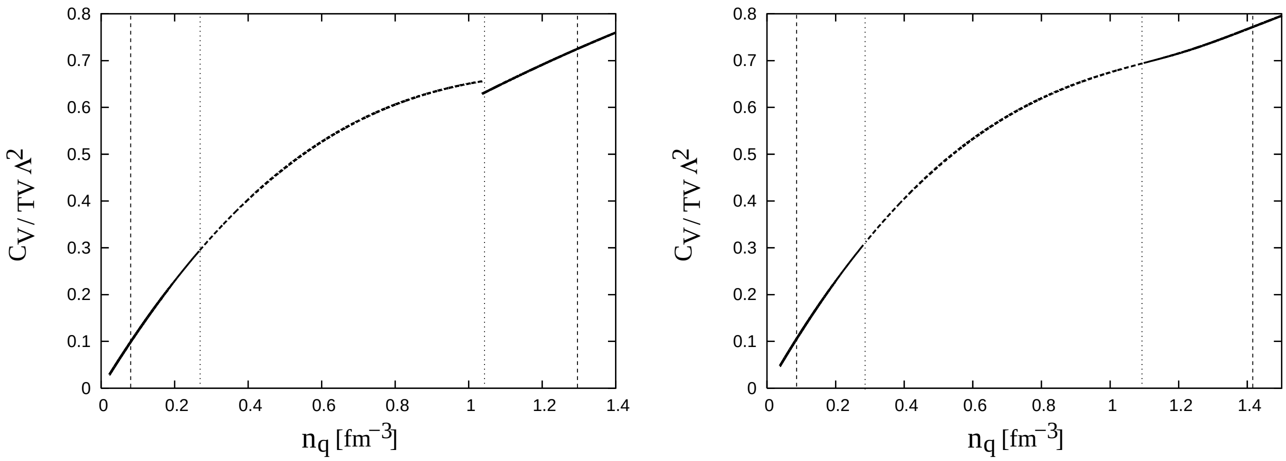

FIG. 7: The specific heat C_V at constant volume and at fixed temperature $T = 30$ MeV in the chiral limit (left panel) and for a finite quark mass $m = 5.6$ MeV (right panel). The vertical dashed-lines indicate the location of the first order phase transition. The dotted-lines show the position of the isothermal spinodal points.

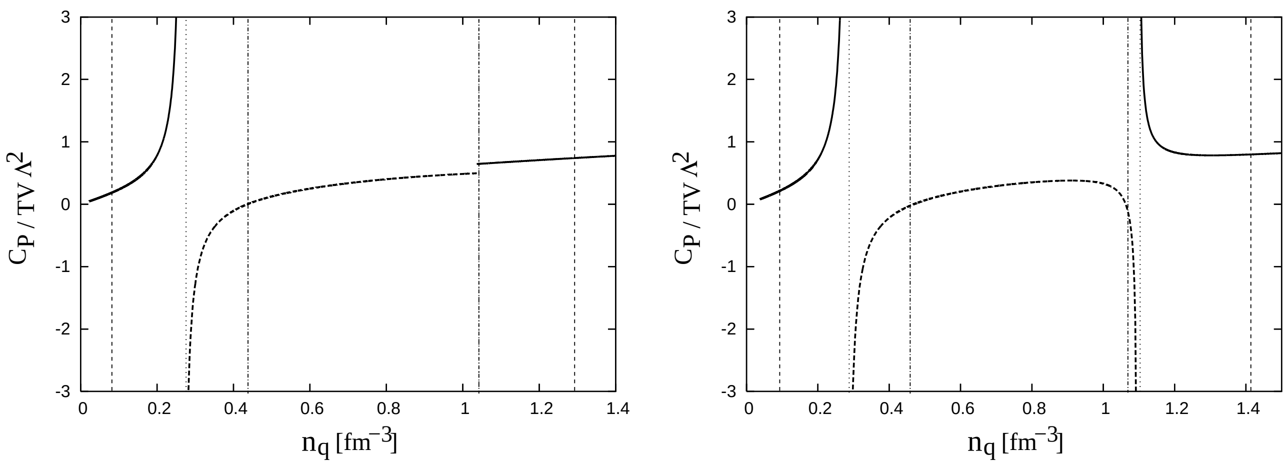

FIG. 8: The specific heat C_P at constant pressure and at fixed temperature $T = 30$ MeV in the chiral limit (left panel) and for a finite quark mass $m = 5.6$ MeV (right panel). The vertical dashed-lines indicate the location of the first order phase transition. The dotted/dashed-dotted lines show the position of the isothermal/isentropic spinodal points.

4. GINZBURG-LANDAU EFFECTIVE THEORY AND CRITICAL EXPONENTS

In the mean filed approximation and near the chiral phase transition the thermodynamic potential obtained in QCD-like chiral models can be described by the Ginzburg-Landau effective theory [26]. Consequently, the mean field critical exponents at the chiral phase boundary can be derived analytically. In earlier studies within this approach the critical exponents of different susceptibilities were obtained assuming that the system appears in equilibrium [19, 21]. In the following we extend the Ginzburg-Landau formalism to account for spinodal phase decomposition in the meta-stable regime of the 1st order transition.

According to the Ginzburg-Landau theory, close to the phase boundary, the thermodynamic potential may be expanded in power series of the order parameter M [26]:

$$\Omega(T,\mu;M) = \Omega_0 - hM + \frac{1}{2}a_2M^2 + \frac{1}{4}a_4M^4 + \frac{1}{6}a_6M^6\,, \tag{4.1}$$

where hM is a term that explicitly breaks the symmetry $M \leftrightarrow -M$. In QCD this corresponds to the quark mass term. The gap equation

$$\Omega'(M) = -h + a_2M + a_4M^3 + a_6M^5 = 0 \tag{4.2}$$

yields the values of the order parameter that extremize the thermodynamic potential. Consider first the case without explicit symmetry breaking, i.e. $h = 0$. Then,

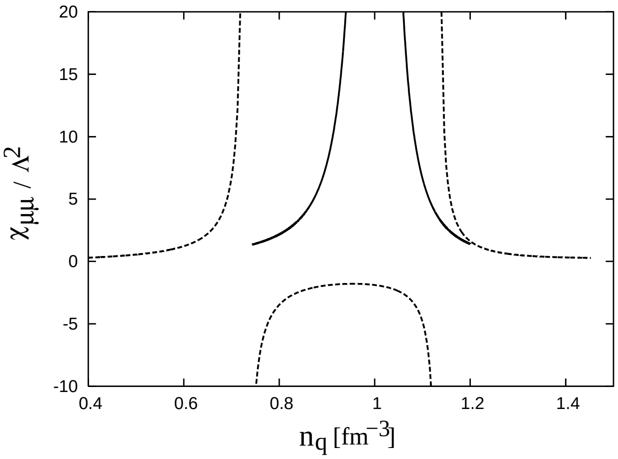

FIG. 9: The net quark number density fluctuations $\chi_{\mu\mu}/\Lambda^2$ normalized to momentum cut-off as a function of the quark number density n_q. The full-line represents the fluctuations at the CEP at constant temperature $T_{\rm CEP} \simeq 80$ MeV. The dashed-line shows the $\chi_{\mu\mu}$ at fixed $T = 70$ MeV corresponding to the 1st order transition.

at a second-order phase transition $a_2 = 0$ and $a_4 > 0$, while at a first order transition $a_2 > 0$, $a_4 < 0$. The parameter a_6 should be positive for stability. Clearly, the TCP can be identified by $a_2 = a_4 = 0$. If $h \neq 0$ and $a_4 > 0$, a change of sign of a_2 corresponds to a cross over transition. We note that in this case it is not possible to uniquely define the position of the transition, since the order parameter M is always non-zero. The endpoint of the first order transition is then called a critical end point (CEP). In order to find the spinodal lines, we need also the second derivative of Ω

$$\Omega''(M) = a_2 + 3a_4M^2 + 5a_6M^4\,. \tag{4.3}$$

The zeroes of the second derivative, $\Omega''(M_0) = 0$, are given by

$$M_0^2 = -\frac{3a_4}{10a_6} \pm \frac{1}{10a_6}\sqrt{9a_4^2 - 20a_2a_6}\,. \tag{4.4}$$

Depending on the values of the parameters, the solutions correspond to inflexion points, or, if M_0 also solves the gap equation, to a point on a spinodal line. We expand the thermodynamic potential around a zero of the second derivative

$$\Omega(m) = \tilde{\Omega}_0 + A_1m + \frac{A_2}{2}m^2 + \frac{A_3}{3}m^3 + \frac{A_4}{4}m^4\,, \tag{4.5}$$

where $m = M - M_0$. One finds

$$\begin{aligned} A_1 &= -h + a_2M_0 + a_4M_0^3 + a_6M_0^5 \\ A_2 &= a_2 + 3a_4M_0^2 + 5a_6M_0^4 = 0 \\ A_3 &= 3a_4M_0 + 10a_6M_0^3 = \pm M_0\sqrt{9a_4^2 - 20a_2a_6} \\ A_4 &= a_4 + 10a_6M_0^2 = -2a_4 \pm \sqrt{9a_4^2 - 20a_2a_6}\,. \end{aligned} \tag{4.6}$$

At a spinodal line the gap equation is satisfied, i.e., $A_1 = 0$. Thus, close to a spinodal line,

$$\begin{aligned} A_1 &= a_1(T - T_0) + b_1(\mu - \mu_0) \\ A_2 &= a_2(T - T_0) + b_2(\mu - \mu_0)\,, \end{aligned} \tag{4.7}$$

while the coefficient A_3 is non-zero, and can be taken to be constant over the small range of temperatures and chemical potentials considered. In the gap equation for a point close to the spinodal line $\mu \simeq \mu_0$ (for definiteness we set $T = T_0$),

$$A_1 + A_2m + A_3m^2 + A_4m^3 = 0\,, \tag{4.8}$$

we assume that $m \sim \pm|\mu - \mu_0|^\alpha$, with [#4] $0 < \alpha < 1$. For small $|\mu - \mu_0|$, the leading terms of (4.8) are then $A_1 + A_3m^2 = 0$, yielding $\alpha = 1/2$. At the critical end point also $A_3 = 0$, so the leading terms in the gap equation are $A_1 + A_4m^3 = 0$, and correspondingly $\alpha = 1/3$. The singular part of the baryon number susceptibility is given by

$$\chi_{\mu\mu}^{sing} = -\frac{\partial^2\Omega}{\partial\mu^2} = -b_1\frac{\partial m}{\partial\mu} \sim |\mu - \mu_0|^{-\gamma}\,, \tag{4.9}$$

with $\gamma = 1/2$ at the spinodal lines and $\gamma = 2/3$ at the CEP. Thus, the singularities of the two spinodal lines conspire to yield a somewhat different critical exponent at the CEP. In the chiral limit, $\alpha = 1/2$ at the spinodal lines and the corresponding critical exponent is $\gamma = 1/2$. Finally, at the TCP $\alpha = 1/4$, but the critical exponent is unchanged, since here $M = 0$ and

$$\chi_{\mu\mu} \sim M\frac{\partial M}{\partial\mu} \sim \frac{\partial M^2}{\partial\mu} \sim |\mu - \mu_0|^{-1/2}\,. \tag{4.10}$$

Thus, in the chiral limit the critical exponents of the baryon number susceptibility at the spinodal lines and at the TCP are identical, while for finite quark masses the corresponding exponents differ. The critical and the universal properties at the phase boundary can be also studied considering the fluctuations of the order parameter. They are characterized by the chiral susceptibility, χ_{mm} defined as the second order derivative of thermodynamic potential with respect to the quark mass

$$\chi_{mm} = -\frac{\partial^2\Omega}{\partial m^2}. \tag{4.11}$$

Figure 11 shows the change of the chiral susceptibility near the critical end point and along the spinodal lines in the chiral limit and for the finite value of the quark masses. In the chiral limit the behavior of χ_{mm} as a function of $t = |(\mu - \mu_c)/\mu_c|$ differs from that shown in Fig. 10 for the net quark number density fluctuations $\chi_{\mu\mu}$.

[#4] The assumption $|\alpha| > 1$ does not yield a consistent solution of (4.8).

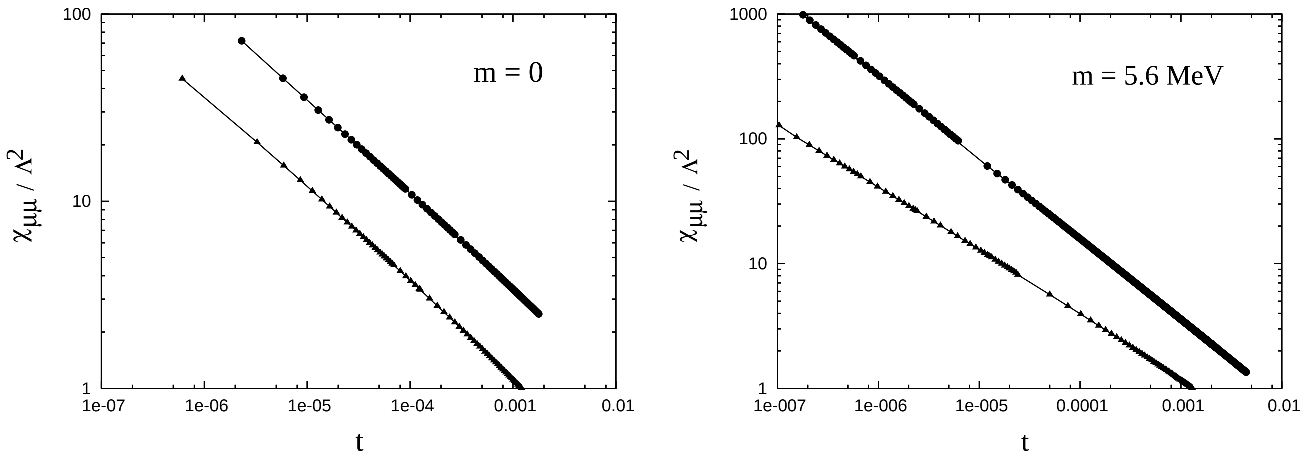

FIG. 10: The net quark number susceptibility in the vicinity of the TCP (left panel) and CEP (right panel) as a function of the reduced quark chemical potential $t = (\mu - \mu_c)/\mu_c$ at fixed T. The filled circle (●) denotes the results calculated at $T = T_{\rm TCP/CEP}$ and the filled triangle (▲) at $T = 30$ MeV $< T_{\rm TCP/CEP}$ corresponding to the first order transition.

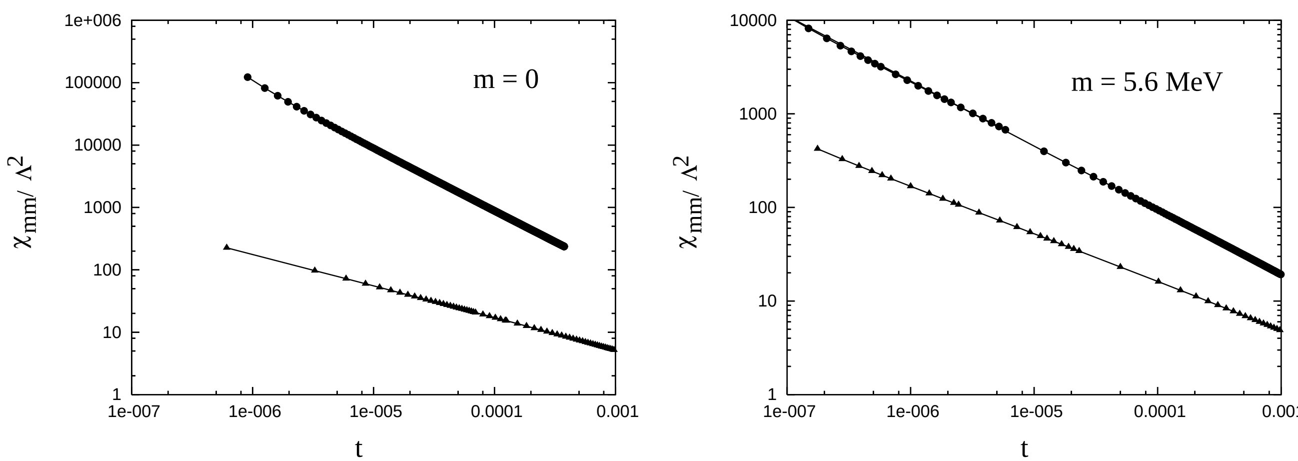

FIG. 11: The chiral susceptibility in the vicinity of the TCP and spinodals in the chiral limit (left panel) and at finite quark mass (right panel) as a function of the reduced quark chemical potential $t = (\mu - \mu_c)/\mu_c$ at fixed T. The filled circle (●) denotes the results calculated at $T = T_{\rm TCP/CEP}$ and the filled triangle (▲) at $T = 30$ MeV $< T_{\rm TCP/CEP}$ corresponding to the first order transition.

First, the critical exponents at TCP and along spinodals do not coincide. Second, the critical exponent γ at the TCP is now equal to unity instead of $\gamma = 1/2$ whereas at spinodals it still remains the same as for $\chi_{\mu\mu}$. On the other hand, at finite quark mass the critical exponents at the CEP and at the spinodals for χ_{mm} are the same as found for $\chi_{\mu\mu}$. The above properties are to be expected in mean field dynamics because of the following relation

$$\chi_{\mu\mu} \simeq \chi_{\mu\mu}^{reg} + M^2 \chi_{mm}, \qquad (4.12)$$

that connects $\chi_{\mu\mu}$ with χ_{mm} and the dynamical quark mass M. The first term χ^{reg} corresponds to a non-singular contribution to the quark number fluctuations. In the chiral limit, when approaching the TCP along any paths being not asymptotically tangential to the critical line the order parameter $M^2 \sim t^{1/2}$ and at the O(4) line $M^2 \sim t^1$ [14]. The corresponding exponents of χ_{mm} are $\gamma = 1$, what explains through Eq. (4.12) the critical exponents found in the Fig. 11-left. For the first-order transition in the chiral limit and for the finite quark mass the M^2 is always finite, consequently the critical exponents of $\chi_{\mu\mu}$ and χ_{mm} are identical as seen in Fig. 11.

5. SUMMARY AND CONCLUSIONS

Considering deviations from an idealized equilibrium picture of the first order chiral phase transition by in-

cluding spinodal instabilities, we have explored the critical behavior of the fluctuations of conserved charges and the specific heat in the NJL model in mean field approximation. We have studied the properties these observables in the chiral limit and for finite vale of the quark chemical potential. We showed that the charge fluctuations diverge along the isothermal spinodal lines of the first order chiral phase transition independently on the value of quark masses. Accompanied by the singularities of the susceptibilities, the specific heat at constant pressure also diverges. This is in contrast to an equilibrium transition where the susceptibilities are finite and only at the TCP/CEP diverge. This implies that large fluctuations of the density would be a signal not only for the existence of the CEP or TCP but also of a non-equilibrium first order transition. The above is especially relevant to the current and future heavy-ion experiments when considering a possible signal for a first order chiral phase transition.

We also showed that in the chiral limit the critical exponents of the net quark number susceptibility $\chi_{\mu\mu}$ are identical at the TCP and at the isothermal spinodals. In the mean field approximation the critical properties of the net quark number fluctuations were found to be governed by a common critical exponent $\gamma = 1/2$. On the other hand at finite quark masses the exponents are different indicating a change of the universality class. At the spinodals the critical exponents for $m \neq 0$ stays to be $\gamma = 1/2$. However, at the CEP it changes from $\gamma = 1/2$ at $m = 0$ to $\gamma = 2/3$ for $m \neq 0$. These values of the critical exponents were calculated numerically in the NJL model and also confirmed by the analytic studies of an effective Ginzburg-Landau theory. The above results indicates that the singularities of $\chi_{\mu\mu}$ at the TCP and CEP are a remnant of divergent fluctuations along the two spinodal branches.

The calculations were performed within the NJL model under mean field dynamics. However, the appearance of the singularities in the quark fluctuations and specific heat comes from the thermodynamic relations which connect the pressure derivatives with different charge susceptibilities. Thus, divergent properties of charge susceptibilities and the specific heat in the presence of spinodal instabilities are quite general, being independent on the specific formulation of the chiral Lagrangian. This is also the case for the fluctuation critical exponents at the spinodals and their relation to the critical properties at TCP and CEP that should be valid for all QCD like chiral models under mean field approximation. It is a further challenge to verify the influence of the quantum and thermal fluctuations on the critical medium properties in the presence of spinodal phase separation.

Acknowledgments

We acknowledge stimulating discussions with J. Randrup, M. Stephanov and S. Toneev. The work of B.F. and C.S. was supported in part by the Virtual Institute of the Helmholtz Association under the grant No. VH-VI-041. C.S. also acknowledges partial support by DFG cluster of excellence "Origin and Structure of the Universe". K.R. acknowledges partial support of the Polish Ministry of National Education (MENiSW) and DFG under the "Mercator program".

[1] P. Chomaz, M. Colonna and J. Randrup, Phys. Rept. **389**, 263 (2004).
[2] H. Heiselberg, C. J. Pethick and D. G. Ravenhall, Phys. Rev. Lett. **61**, 818 (1988); Annals Phys. **223**, 37 (1993).
[3] D. Bower and S. Gavin, J. Heavy Ion Physics **15**, 269 (2002). J. Randrup, J. Heavy Ion Physics **22**, 69 (2005).
[4] V. Koch, A. Majumder and J. Randrup, Phys. Rev. C **72**, 064903 (2005).
[5] J. Randrup, Phys. Rev. Lett. **92**, 122301 (2004).
[6] J. Polonyi, hep-th/0509078.
[7] K. Paech, H. Stoecker and A. Dumitru, Phys. Rev. C **68**, 044907 (2003); K. Paech and A. Dumitru, Phys. Lett. B **623**, 200 (2005).
[8] C. Sasaki, B. Friman and K. Redlich, Phys. Rev. Lett. **99**, 232301 (2007).
[9] Y. Nambu and G. Jona-Lasinio, Phys. Rev. **122**, 345 (1961); Phys. Rev. **124**, 246 (1961).
[10] For reviews and applications of the NJL model to hadron physics, see e.g., U. Vogl and W. Weise, Prog. Part. Nucl. Phys. **27**, 195 (1991); S. P. Klevansky, Rev. Mod. Phys. **64** (1992) 649; T. Hatsuda and T. Kunihiro, Phys. Rept. **247**, 221 (1994); M. Buballa, Phys. Rept. **407**, 205 (2005).
[11] T. Kunihiro, Phys. Lett. B **271** 395 (1991).
[12] T. Hatsuda and T. Kunihiro, Prog. Theor. Phys. **74**, 765 (1985).
[13] O. Scavenius, A. Mocsy, I. N. Mishustin and D. H. Rischke, Phys. Rev. C **64**, 045202 (2001); A. Mocsy, F. Sannino and K. Tuominen, Phys. Rev. Lett. **92**, 182302 (2004).
[14] C. Sasaki, B. Friman and K. Redlich, Phys. Rev. D **75**, 054026 (2007).
[15] M. Stephanov, Acta Phys.Polon. B **35**, 2939 (2004); Prog. Theor. Phys. Suppl. **153**, 139 (2004); Int. J. Mod. Phys. A **20**, 4387 (2005).
[16] H. Fujii, Phys. Rev. D **67**, 094018 (2003). H. Fujii and M. Ohtani, Phys. Rev. D **70**, 014016 (2004).
[17] M. A. Stephanov, K. Rajagopal and E. V. Shuryak, Phys. Rev. Lett. **81**, 4816 (1998).
[18] Y. Hatta and M.A. Stephanov, Phys. Rev. Lett. **91**, 102003 (2003)
[19] C. Sasaki, B. Friman and K. Redlich, Phys. Rev. D **75**, 074013 (2007).
[20] K. Redlich, B. Friman and C. Sasaki, J. Phys. G **32**, S283 (2006); J. Phys. G **34**, S437 (2007). J.Phys.G34:S437-444,2007.

[21] Y. Hatta and T. Ikeda, Phys. Rev. D **67**, 014028 (2003).
[22] B. J. Schaefer and J. Wambach, Phys. Rev. D **75**, 085015 (2007).
[23] P. Chomaz and F. Gulminelli, Nucl. Phys. A **647**, 153 (1999).
[24] M. Schmidt, R. Kusche, T. Hippler, J. Donges, W. Kronmuller, B. von Issendorff and H. Haberland, Phys. Rev. Lett. **86** (2001) 1191.
[25] M. D'Agostino *et al.*, Phys. Lett. B **473**, 219 (2000).
[26] L.D. Landau and E.M. Lifshitz, *Statistical Physics*, Course of Theoretical Physics, Vol. 5, (Pergamon Press, New York, 1980) Chapter XIV.